processes

MDPI

Article

Numerical Simulation and Process Enhancement of the Hydrolysis of 2-Chlorobenzal Chloride

Fei Li [1,2], Liang Dong [3], Shenghu Yan [2,4,*], Yue Zhang [2], Jianwu Liu [2,4], Wenping Tao [3], Lichun Nian [3] and Shuangcheng Fu [5]

[1] School of Petrochemical Engineering, Changzhou University, Changzhou 213164, China; 20085600324@smail.cczu.edu.cn
[2] Continuous Flow Engineering Laboratory of National Petroleum and Chemical Industry, Changzhou 213164, China; zyjs@cczu.edu.cn (Y.Z.); liujianwu@cczu.edu.cn (J.L.)
[3] Changzhou Chemical Co., Ltd., China Salt Group, Changzhou 213200, China; donglianghsf@chinasalt.com.cn (L.D.); taowpch@chinasalt.com.cn (W.T.); nianlcch@chinasalt.com.cn (L.N.)
[4] School of Pharmacy, Changzhou University, Changzhou 213164, China
[5] School of Mechanical Engineering and Rail Transit, Changzhou University, Changzhou 213164, China; fushuangcheng@cczu.edu.cn
* Correspondence: ysh@cczu.edu.cn

Abstract: Hydrolysis of 2-Chlorobenzal chloride is the primary production method of 2-chlobrobenzal dehyde in industry, but the reactor technologies and reaction processes of this method are traditional and underdeveloped, in which the dichotomous leaf hydrolysis agitator is commonly used, resulting in low efficiency during the hydrolysis process. In this article, ANSYS software was utilized to enhance the hydrolytic reactors used in industrial production by simulating and analyzing the dispersion characteristics of droplets in the reactor. The particle size distribution of dispersed phase droplets and the Sauter mean diameter (D_{32}) were used to characterize the dispersion effect, and the dispersion characteristics of the dichotomous leaf agitator and the three-bladed back-curved impeller, three-bladed propeller impeller, open turbine impeller, and crescent impeller were compared and studied. The results showed that there was a log-linear relationship between the D_{32} of the dispersed phase and the stirring speed in different systems; the number of tiny droplets in the three-bladed back-curved impeller system increased remarkably, and the droplets size distribution width decreased significantly, achieving mass transfer enhancement in the hydrolysis reaction system. The reliability of the simulation results was verified by the measurement experiment using the Sauter mean diameter (D_{32}) of dispersed phase droplets. The results showed that the Sauter mean diameter (D_{32}) variation trend is consistent with that of the simulation, and the error between them is less than 10%. A lab-scale hydrolytic reactor was designed and produced based on the scheme of an industrial hydrolytic reactor equipped with a three-bladed back-curved impeller, the effect of the hydrolytic reaction was verified, and the process conditions were strengthened under the same conditions. The results showed that, compared with the case in the reactor using a dichotomous leaf hydrolysis agitator at the same reaction temperature and catalyst conditions, the reaction time of hydrolysis completion reduced to 58.33% at the lab-scale, and to 63.89% at the industrial-scale at the stirring rate of 446 r/min, using a three-bladed back-curved impeller. These results provide a technical scheme and a basis for process strengthening for improving the production efficiency of 2-chlorobenzaldehyde production equipment in industry.

Keywords: 2-chlorobenzal chloride; hydrolysis reactor; numerical simulation; mixing propeller; process enhancement

Citation: Li, F.; Dong, L.; Yan, S.; Zhang, Y.; Liu, J.; Tao, W.; Nian, L.; Fu, S. Numerical Simulation and Process Enhancement of the Hydrolysis of 2-Chlorobenzal Chloride. *Processes* **2023**, *11*, 945. https://doi.org/10.3390/pr11030945

Academic Editor: Pavel Mokrejš

Received: 21 February 2023
Revised: 16 March 2023
Accepted: 17 March 2023
Published: 20 March 2023

1. Introduction

2-Chlorobenzaldehyde is an important derivative of toluene chloride and an essential intermediate in synthesizing pharmaceuticals, pesticides, and dyes. 2-Chlorobenzaldehyde

can be synthesized by multiple methods, such as the hydrolysis of 2-chlorobenzal chloride, the oxidation of chlorobenzyl alcohol, the indirect electrochemical oxidation of chlorotoluene, and the direct oxidation of chlorotoluene. Among these, the hydrolysis of 2-chlorobenzal chloride is the primary method for the industrial production of 2-chlorobenzaldehyde in prominent areas of China, India, etc. [1]. However, this method causes issues such as low equipment efficiency due to the under-optimized reactor structure design and the low efficiency of the reaction process due to unstrengthened processing conditions. A systematic study of the reactor and process conditions to improve the efficiency of the hydrolysis reaction of 2-chlorobenzal chloride demonstrates research significance and practical value.

CFD techniques have been widely used in recent years in the fields of chemical synthesis [2–4] and polymerization [5,6], and these techniques can perform structural optimization by simulating the flow state of the fluid in the reactor [7]. Most of the 2-chlorobenzal chloride hydrolysis reactions in the industry are currently carried out in kettle-type reactors [8], which are equipped with diagonal-blade stirring paddles for stirring and mass transfer. The stirring paddle has a weak ability to refine the droplets of the dispersed phase in the liquid–liquid nonhomogeneous phase. Therefore, an improved design of the stirring paddle is needed to enhance the outward diffusion of the liquid droplets into the continuous phase, increase the phase contact area, promote mass transfer, and improve the reaction efficiency.

Fredrik [9] studied a liquid-liquid system with aqueous sodium iodide as the continuous phase and silicone oil as the dispersed phase. The effect of the volume fraction of the dispersed phase on the flow field showed that the volume fraction of the dispersed phase significantly influences the fluid velocity and the degree of turbulence. Drumma et al. [10] used n-heptane as the dispersed phase and a 44% mass fraction of the propanetriol–water mixture as the continuous phase. The vessel's single-phase and two-phase flow fields were simulated using Fluent software, and the numerical simulation results agreed with the results of the experiments. The results showed that the simulation method predicted the single-phase and two-phase flow fields in the turntable tower favorably. Lamberto et al. [11,12] investigated the effect of rotational speed on the flow field. The results showed that changing the rotational speed can disturb the flow field, and frequent disturbance in the flow field can reduce the formation of the mixing segregation zone, which increases the area of chaotic mixing in the flow field and facilitates the mixing efficiency. Eastwood C. D. et al. [13] studied the fragmentation of non-mutually soluble fluid particles in typical turbulent flows. The results showed that the fragmentation frequency of fluid particles at low Weber numbers is proportional to the large-scale turbulence characteristics.

In addition, the process conditions of the hydrolysis of 2-chlorobenzal chloride in the current industry are not enhanced, which results in an inefficient reaction process. Therefore, it is necessary to conduct in-depth research on the temperature of the hydrolysis reaction, catalyst concentration, and stirring rate of the operating parameters to improve the efficiency of the hydrolysis of 2-chlorobenzal chloride.

In this study, CFD numerical simulation is used to enhance the design of the diagonal-bladed stirring paddle currently configured in an industrial reactor for hydrolysis of 2-chlorobenzal chloride. The dispersion characteristics of the diagonal-bladed type, three-blade back-curved type, three-blade propeller type, open turbine type, and crescent type stirring paddles are comparatively studied. The dispersion effect is characterized by the particle size distribution and the Sauter mean diameter (D_{32}) of the dispersed phase droplets. The optimal structural parameters of the hydrolysis reactor were determined, and a lab-scale hydrolysis reactor was designed and produced. Water and 2-chlorobenzal chloride are used as raw materials, and the conversion rate of 2-chlorobenzal chloride is used as the reference index. The optimal condition of the lab-scale hydrolysis of 2-chlorobenzal chloride is determined by a single-factor test and orthogonal experiment optimization. The effect of the industrial-scale hydrolysis of 2-chlorobenzal chloride is studied after applying

the optimal lab-scale technical solution. This can provide a technology scheme for process enhancement for the increased production capacity of 2-chlorobenzaldehyde in industry.

2. Material and Methods

2.1. Experimental Materials

The materials used in the experiment are 2-Chlorobenzal chloride (purity $\geq$ 98%, Changzhou Chemical Co., Ltd., China Salt Group, Changzhou, China), and Alkyl alcohol amine (purity $\geq$ 99%, Chinasun Specialty Products Co., Ltd., Changshu, China).

2.2. Instruments and Equipment

The equipment used in this experiment is as follows: C-MAG HS 10 IKAMAG® (IKA WORKS GUANGZHOU, Guangzhou, China); JB40-C Mechanical Mixer (Shanghai Biaoben Model Factory, Shanghai, China); GC-7890B GC System (Agilent Technologies (China) Co., Ltd., Beijing, China); and Phantom®UHS-12 Ultrahigh-speed cameras (Vision Research Inc., Wayne, NJ, USA); 0.53 mm $\times$ 30 m CSKJ CS-05 Capillary Column (Changzhou University, Changzhou, China).

2.3. Methods

2.3.1. Geometric Model and Grid Partition

Enamel reactors are used for the hydrolysis of 2-chlorobenzal chloride in industrial production [14,15]. This type of reactor cavity is surrounded by a cylinder, including upper and lower standard elliptical heads, with a single kettle volume of 10,000 L, and its structure is shown in Figure 1. In the hydrolysis kettle, the dichotomous leaf agitator is installed near the bottom, and the liquid level is controlled at 2750 mm in the process of the hydrolysis of 2-chlorobenzal chloride. Considering the dosage of the reaction raw materials of the hydrolysis of 2-chlorobenzal chloride and the convenience of simulation calculation in the later stage, the size of lab-scale reactor is reduced according to 27.5:1, referring to the size of industrial-scale reactor in Figure 1. The volume of the lab-scale reactor is 250 mL, and the main structural parameters of the kettle and the stirring paddle are shown in Figure 2.

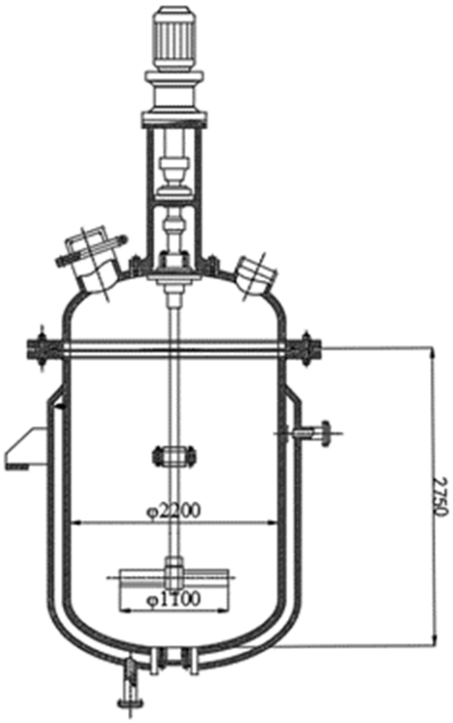

Figure 1. Industrial-scale reaction kettle.

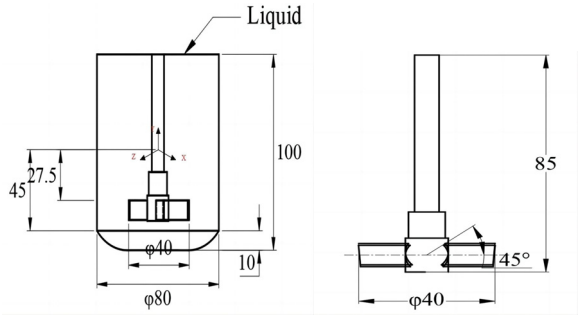

Figure 2. Lab-scale stirred reactor.

A dichotomous leaf agitator is used in the industrial production of the hydrolysis reaction, as shown in Figure 3, B_0. In actual production, it was found that the stirring paddle had a weak shearing effect and provided low radial flow energy. It is necessary to optimize the structural form of the stirring paddle of the hydrolysis reactor for our research. Radial flow mixing paddles can be of the crescent type, straight-blade type, back-bending type, propulsion type, open turbine type, or disc turbine type. Because typical forms are the backbend, propulsion, open turbine, and crescent type, this paper refers to the typical mixing paddle structure. A series of stirring paddles, applicable to the lab-scale reactor for hydrolysis shown in Figure 2, is designed, as shown in Figure 3 for B_1, B_2, B_3, and B_4.

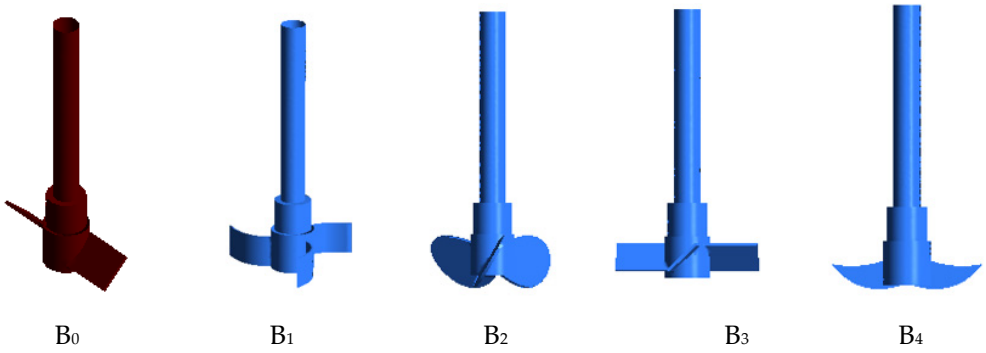

Figure 3. Schematic diagram of five blade structures.

The ANSYS-ICEM software is used for mesh division. The fluid domain is divided into two parts: the rotating region of the agitator blade and the static region, except for the rotating domain. The rotating domain and the static domain are discretized by tetrahedral mesh, and the local mesh is encrypted at the area of the blade. The mesh model is shown in Figure 4.

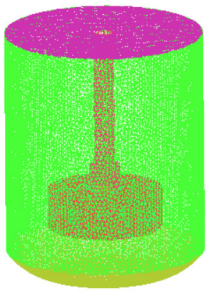

Figure 4. Meshing of the reaction kettle.

In the study, four types of dichotomous leaf agitators with different grid numbers are used for the research of grid independence at 150 r/min. The velocity vector field of the kettle is compared and analyzed within X = 0 mm, Y = −20 mm, and Z from −40 mm to

40 mm at 10 s. The results are shown in Figure 5, where N is the number of grids divided. A similar trend is shown through the simulation results of flow field velocity with four different grid numbers, mainly the sampling curve N = 100 w and the sampling curve N = 67 w. However, there is a more significant error between the sampling curve N = 20 w and the sampling curve N = 42 w at lower grid density. The grid density of N = 67 w is preferred, because it can meet the requirements of grid independence and ensure reliability, reducing both the calculation and consumption time.

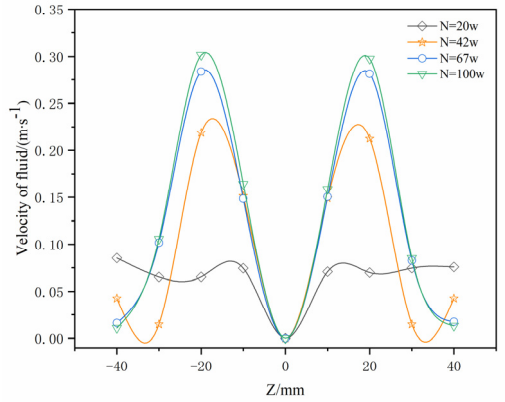

Figure 5. Grid independence.

2.3.2. Physical Model and Governing Equation

The reaction kettle is composed of an aqueous phase and a 2-chlorobenzal chloride oil phase, regardless of the gas phase and the adhesion process of 2-chlorobenzal chloride on the kettle wall. The physical models selected for the calculation based on the above assumptions are mainly the general multiphase model, turbulence model, and population balance model. The Eulerian two-fluid flow model [16] is used for the general multiphase model, and the RNG k-ε turbulence model [17] is used for the turbulence model. The Luo fragmentation model and the Luo aggregation model are chosen for this study because of the factors of fragmentation and aggregation of the dispersed phases in different stirred systems [18]. The Eulerian and PBM models [16] are coupled in Fluent 19.0 software, and the particle size distribution of the dispersed phase in different stirred systems is simulated by using the RNG k-ε turbulence model.

In the Eulerian two-fluid flow model, the liquid-liquid phases are assumed to be continuous media, respectively, and the two phases simultaneously fill the entire flow field. The oil phase of 2-chlorobenzyl chloride is used as the discrete phase, and the water phase is the continuous phase in the process of numerical simulation. The continuous and dispersed phases are regarded as continuous media. The Eulerian two-fluid model established the equation of continuity and the momentum equation for each phase, and the governing equation of the two phases is shown in Equations (1) and (2) [19].

Equation of continuity:

$$\frac{\partial_{\rho_k}\alpha_k}{\partial_t} + \nabla\cdot(\rho_k\alpha_k u_k) = 0 \quad (1)$$

Momentum equation:

$$\frac{\partial_{\rho_k}\alpha_k u_k}{\partial_t} + \nabla\cdot(\rho_k\alpha_k u_k u_k) = -\alpha_k\nabla P' + \nabla\cdot\left[\alpha_k\mu_{eff,k}\left(\nabla u_k + \nabla {u_k}^T\right)\right] + F_{g,1} + \rho_k\alpha_k g \quad (2)$$

where k is the liquid phase, α is phase volume fraction, ρ is the density, u is the velocity, P' is the corrected pressure, μ is the viscosity, g is the gravitational acceleration, and $F_{g,1}$ is the liquid–liquid interphase force.

2.3.3. Model Solving

Since CFD technology was introduced into the study of stirred tank flow fields by Harvey and Greaves [20,21], many stirring simulation methods have evolved. At present, the multiple reference frame (MRF) methods and the sliding grid (SG) methods are widely regarded as the most appropriate approaches to simulate impeller rotation [22].

The MRF method [7] is frequently used in simple mixed models because of its low resource requirements and efficient processing capacities compared with SG. Therefore, the MRF method is used in this study to simulate the fluid flow state during 2-chlorobenzal chloride hydrolysis.

The calculation region is divided into two regions, the moving region and the static region, for the numerical solution. The dynamic region is set to 100~350 r/min for rotating motion, and the static region remains static. The agitator and stirring shaft are set as motion boundaries, and the type is a wall. The relative speed is set to 0, because the agitator located in the moving area moves with the rotation of the moving region. The stirring shaft, which is located in the static area, actively rotates relative to this region, the rotational speed is the same as that in the dynamic region, and the wall of the kettle is set to the static wall. Then, the PBM model is added and solved by the uniform discretization method. Finally, the SIMPLE algorithm is used to solve the relationship of pressure-rate coupling, the differential format is used in the second-order windward format, the residual errors of the model monitor are set to 10^{-5}, and the time step of the nonsteady-state calculation is set as 0.01 s. We then observe whether the convergence of the residual curve in each step of transient computation reached the residual value programmed. The flow field results are obtained after the convergence of the model. The physical parameters of the substances involved in the solution of the model are shown in Table 1.

Table 1. The physical properties of computational mediums.

Material	Density/(kg/m^3)	Viscosity/(kg/m·s)
water	998.2	1.003×10^{-3}
2-chlorobenzal chloride	1281.32	7.356×10^{-4}

2.3.4. Selection of Reaction Vessel Simulation Conditions

At a distance of 15 mm from the bottom of the kettle, the stirring paddle diameter was 40 mm, and the stirring rate was 150~300 r/min. The particle size distribution and D_{32} of the dispersed phase in the stirring system of B_0, B_1, B_2, B_3, and B_4 were simulated to study the dispersion characteristics of the dispersed phase (2-chlorobenzal chloride) in different stirring systems. The particle size distribution of the dispersed phase droplets and the Sauter mean diameter (D_{32}) were used to represent the dispersion effect and to determine the best mixing impeller.

2.3.5. Design and Production of the 2-Chlorobenzal Chloride Hydrolysis Reaction Kettle

The reaction kettle with a height of 150 mm, an inner diameter of 80 mm, and a thickness of 10 mm is made of glass, and the optimal stirring paddle is determined based on the results of the simulated parameters.

2.3.6. 2-Chlorobenzal Chloride Hydrolysis Reaction Conditions

First, 2-chlorobenzal Chloride, water with a mol ratio of 1:2.4, 2-chlorobenzal chloride, and phase transfer catalyst alkyl alcohol amine with a mol ratio of 25:1 were added to the hydrolysis reaction kettle, mixed sufficiently, and the temperature was increased to 105 °C. The effects of stirring paddles B_0, B_1, B_2, B_3, and B_4 on the conversion rate of 2-chlorobenzal chloride at different stirring rates were studied under these conditions.

2.3.7. Optimization of the 2-Chlorobenzal Chloride Hydrolysis Process

The optimal stirring paddle suitable for the hydrolysis process of 2-chlorobenzal chloride was determined based on a univariate test with reaction time (A) and stirring rate (B) as independent variables and the conversion rate of 2-chlorobenzal chloride as the response value. A two-factor, four-level experimental design was carried out for stirring paddles B_0, B_1, B_2, B_3, and B_4. Taking stirring paddle B_1 as an example, its test factors and level design are shown in Table 2. The B_0, B_2, B_3, and B_4 stirring paddles are designed according to the same method.

Table 2. Factors and their coded and actual levels used in the Box–Behnken design.

Factors	Level		
	−1	**0**	**1**
A. Reaction time/h	15	20	25
B. Stirring rate/(r/min)	150	300	450

Note: B_0, B_1, B_2, B_3, B_4 are the dichotomous leaf agitator type, three-blade back-curved type, three-blade propulsion type, open turbine type, and crescent-type mixing paddle, respectively.

2.3.8. Measurement of the Conversion Rate of 2-Chlorobenzal Chloride

The transformation of 2-chlorobenzal chloride was determined by the measurement of the area and content of the substance through gas chromatography area normalization. Furthermore, it was essential to utilize the area normalization method to quantify the results. First, 1 mL of the hydrolysis reaction liquid was extracted, a little lye was added, and then the upper water and lower oil phases were obtained by static stratification. Then, 0.5 µL of oil phase was extracted by micro syringe, and the percentage content of the sample was obtained through the separation of the chromatographic column, signal acquisition, and data processing for the chromatographic workstation. The gas chromatography analysis conditions are shown in Table 3.

Table 3. The gas chromatography analysis conditions.

Type of Carrier Gas	Value of Pressure/(MPa)	Type of Temperature	Value of Temperature/(°C)
N_2	0.4	Column	100
H_2	0.2	Detection room	280
		Vaporization room	280

In addition, the determination of the molar correction factor of the gas chromatography needs to be performed before the experiment because the gas chromatography exhibits a certain measurement error. The self-formulated standard solution is used to calibrate the analysis results of the gas chromatography (external standard method). The molar ratio of 2-chlorobenzal chloride to 2-chlorobenzaldehyde of the self-formulated solution, the gas phase peak area ratio, and the molar correction factor are shown in Table 4. The molar ratio of 2-chlorobenzal chloride to 2-chlorobenzaldehyde of the self-formulated solution and gas peak area ratio is fitted by the linear function in Origin software, and the fitting results are shown in Figure 6.

Table 4 shows that the gas chromatography analysis result is higher than the actual value. Therefore, the result of gas chromatography analysis needs to be multiplied by a molar correction factor of 0.9884 in the calculation of the conversion rate of 2-chlorobenzal chloride in subsequent hydrolysis experiments, and the curve fitting result in Figure 6 shows that the experimental results of the gas phase molar correction factor are reliable.

Table 4. The molar ratio of 2-chlorobenzal chloride to 2-chlorobenzaldehyd and the gas peak area ratio.

a	*b*	*a*/*b*	$\overline{a/b}$
8.04	7.4806	1.075	
3.575	3.2791	1.09	
2.213	2.2774	0.972	
1.325	1.39075	0.9527	
0.88	0.82859	1.0620	0.9884
0.6	0.62833	0.9549	
0.3857	0.40447	0.9536	
0.225	0.23823	0.9445	
0.09889	0.11079	0.8909	

Note: $a = {}^{n_s}/_{n_i}$, $b = ({}^{A_s}/_{A_i})$, a/b is the molar correction factor; n_s is the amount of 2-chlorobenzal chloride in the self-formulated solution, n_i is the amount of 2-chlorobenzaldehyde in the self-formulated solution, A_s is the gas peak area of 2-chlorobenzal chloride, and A_i is the gas peak area of 2-chlorobenzaldehyde.

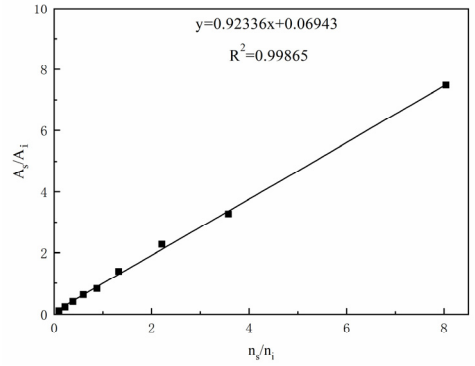

Figure 6. Fitting curve of actual molar ratio of 2-chlorobenzal chloride to 2-chlorobenzaldehyde and the gas peak area ratio.

3. Results and Discussion

3.1. Numerical Simulation and Optimization of Stirring Conditions for the Hydrolysis Reaction of the Lab-Scale Tests

3.1.1. Particle Size Distribution of Dispersed Phase Droplets in Different Stirring Systems

The diameter of the stirring paddle is 1/2 of the diameter of the kettle, i.e., the diameter of the stirring paddle is 40 mm at the height of 15 mm from the bottom of the reactor. The particle sizes of the dispersed phase droplets in five different stirring systems, B_0, B_1, B_2, B_3, and B_4, were simulated at different stirring rates. The simulated particle size distribution is shown in Figure 6.

Figure 7 shows the distribution of the number of dispersed phases in the same interval at different speeds for different stirrers. The particle size distribution of different mixing systems ranged from 0.1 to 12.222 mm. Since the particle size distribution of different mixing systems is mainly concentrated in 0.1 mm, only this particle size is described here. The number of droplets with a particle size of 0.1mm accounted for 24.76%, 29.20%, 32.30%, and 32.90% for the B_0 stirring system in the speed range of 150 r/min to 300 r/min, respectively. The number of droplets with a particle size of 0.1 mm accounted for 53.7%, 61.9%, 67.4%, and 69.2%, respectively, for the B_1 stirring system in the speed range of 150~300 r/min. The number of droplets with a particle size of 0.1 mm accounted for 49.3%, 53.5%, 63%, and 68.8%, respectively, for the B_2 stirring system in the speed range of 150~300 r/min. The number of droplets with a particle size of 0.1 mm accounted for 46.4%, 51.6%, 61.8%, and 64.9%, respectively, for the B_3 stirring system in the speed range of 150 r/min~300 r/min. The number of droplets with a particle size of 0.1 mm accounted for 24.1%, 31.2%, 50.8%, and 57.7% for the B4 stirring system in the speed range of 150~300 r/min, respectively. The percentage of droplets with a particle size of 0.1 mm increases with the speed increase for different stirring systems. Compared with the other

three stirrer systems, the droplets with a particle size of 0.1 mm in the B_1 stirrer system make up a large percentage during different rotating speeds. Therefore, the number of tiny droplets in the B_1 stirrer system is relatively large, and the particle size is more uniform.

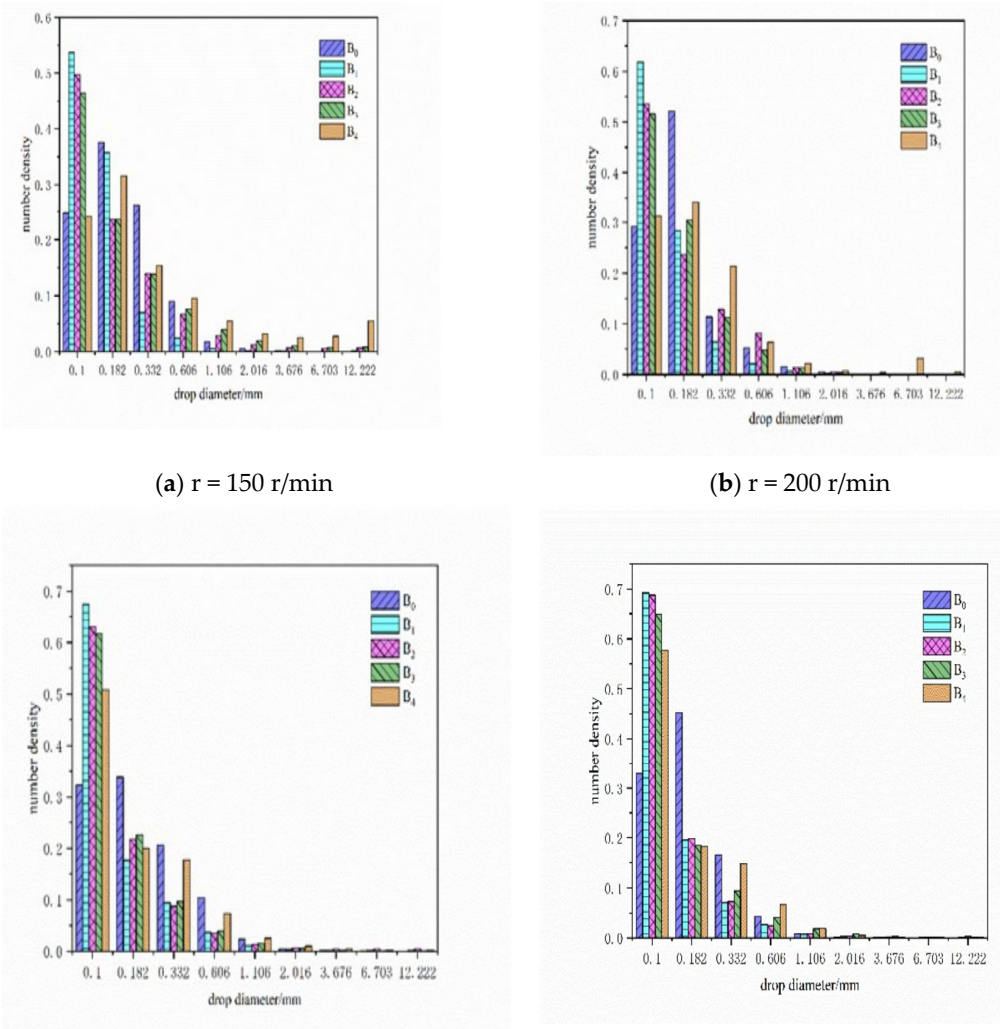

(**a**) r = 150 r/min (**b**) r = 200 r/min

(**c**) r = 250 r/min (**d**) r = 300 r/min

Figure 7. The distribution of dispersed phase droplets in different impeller systems.

3.1.2. Comparison of D_{32} for Different Stirring Systems at Different Speeds

The droplet particle size distribution pattern is generally analyzed by the Sauter mean diameter (SMD), and D_{32} usually expresses the SMD:

$$D_{32} = \frac{\sum n_i d_i^3}{\sum n_i d_i^2} \tag{3}$$

where n is the droplet diameter, and d is the number of droplets.

As shown in Figure 8, the D_{32} values for different stirring systems were fitted, and the linear relationship $lgD_{32} - lgN$ is shown in Equations (4) to (8), where the results of the B_0 stirring paddle fitting were as follows:

$$lgD_{32} = 1.92452 - 0.41363lgN \tag{4}$$

The results of the B_1 stirring paddle fit were as follows:

$$lgD_{32} = 2.55024 - 0.80055lgN \quad (5)$$

The results of the B_2 stirring paddle fit were as follows:

$$lgD_{32} = 2.56277 - 0.78096lgN \quad (6)$$

The results of the B_3 stirring paddle fit were as follows:

$$lgD_{32} = 2.21443 - 0.59231lgN \quad (7)$$

The results of the B_4 stirring paddle fit were as follows:

$$lgD_{32} = 2.18502 - 0.55333lgN \quad (8)$$

As shown in Figure 8, different types of stirring paddles will affect the distribution of droplet size in the reactor. This conclusion is consistent with the findings of Daglas et al. [23]. In addition, D_{32} decreases with the increase in speed for different stirring paddle systems, which is consistent with the findings of Sechremeli et al. [24]. It is also found that the value of D_{32} of the B_1 stirring paddle system is less than that of the other four mixing systems. The analysis suggests that the structure of the B_1 stirring paddle has a more substantial shear-breaking effect on the droplets during fluid mixing than does the structure of the other four stirring paddles.

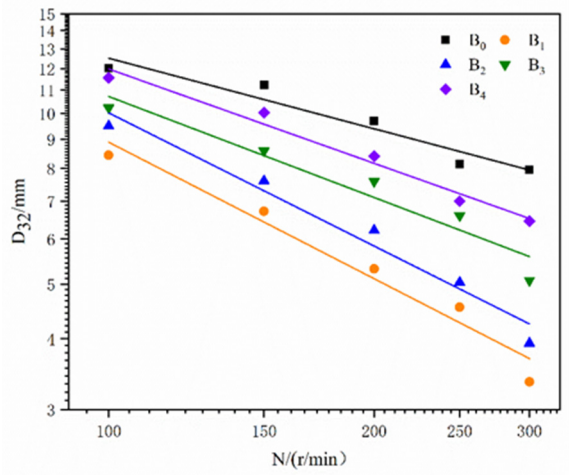

Figure 8. Effect of stirring speed on D_{32}.

3.2. Experimental Measurement of the Diameter of Dispersed Phase Droplets

The average diameter of dispersed phase droplets is measured at a ratio of 1% of the dispersed phase. The clear images can be taken without adding additional staining agents because of the physical and chemical properties of 2-chlorobenzal chloride, which make it appear yellow in color. The speed of the agitator increases from 150 r/min to 200 r/min, 250 r/min, and 300 r/min, in turn, at a constant temperature in every experiment. The high-speed photography method is used to capture the oil phase in the reactor to prevent the aggregation of oil phases from affecting the experiment results. The agitator is designed to stir at a steady speed for 30 min before photographing, and the particle size distribution and the diameter of the dispersed phase droplets in the reactor can be obtained by photography when the system reaches equilibrium. The area of oil droplets is obtained after the Image-J software is used to identify and analyze the oil droplets in the photograph, and the Sauter mean diameter (D_{32}) is calculated. Finally, the experimental data obtained through processing calculation is compared with the simulated data to verify the reliability of the

simulation results. The dispersed phase droplets of the mixing system for B_2, B_3, and B_4 are selected to verify the reliability of the simulation method during the preliminary exploration experiment. The experimental results are shown in Figure 9, and the comparison of the simulated and experimental results is shown in Figure 10.

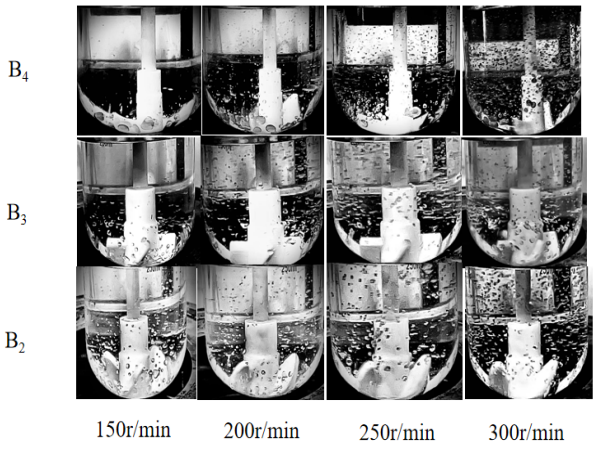

Figure 9. Experimental results of particle size distribution.

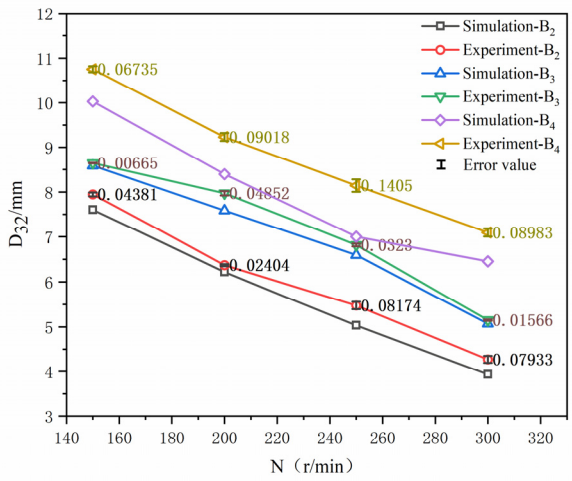

Figure 10. Comparison of simulated and experimental results.

The comparison of simulated and experimental results in Figure 10 shows that the simulated results are lower than the experimental results because the surface tension coefficient is set in the simulation calculation, and the surfactant is not added during the experiment. However, the variation trend of the Sauter mean diameter (D_{32}) experiment is consistent with that of the simulation. The average error between them is less than 10%, indicating that the simulation data is reliable.

3.3. Lab-Scale Validation of Numerical Simulation Results

3.3.1. Effect of Stirring Paddle Type on the Conversion Rate of 2-Chlorobenzal Chloride

The effect of the stirring paddle type on the conversion rate of 2-chlorobenzal chloride at a reaction temperature of 105 °C, with a reaction time of 25 h and a stirring rate of 150 r/min, is shown in Figure 11. Before the hydrolysis reaction conditions were enhanced, the reaction time of hydrolysis completion was approximately 36 h using the B_0 stirring paddle. As seen in Figure 11, the conversion rate of 2-chlorobenzal chloride per unit of time was significantly higher than that of the other four stirring paddle types using the B_1 stirring paddle simultaneously, which required approximately 25 h to complete the reaction. The analysis shows that the droplet size of the dispersed phase is smaller using

the B_1 stirrer than the other four types of stirrers, resulting in a larger surface area than that of the other four types of stirrers so that the interphase mass transfer process is enhanced and the time of hydrolysis reaction is reduced. This is consistent with the results of the previous simulations of the dispersion characteristics in the hydrolysis reactor; thus, the B_1 stirring paddle was chosen.

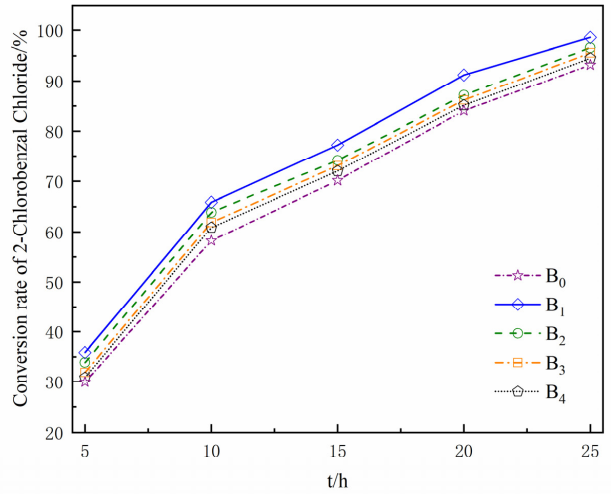

Figure 11. Effect of stirring paddle type on the conversion rate of 2-chlorobenzal chloride.

3.3.2. Effect of Stirring Rate on the Conversion Rate of 2-Chlorobenzal Chloride

The stirring rate is one of the essential factors affecting the hydrolysis reaction speed. At a reaction temperature of 105 °C, a reaction time of 20 h, and a B1 stirring paddle were selected. The effect of the stirring speed on the conversion rate of 2-chlorobenzal chloride is shown in Figure 12. As shown in Figure 12, the reaction proceeds faster as the stirring rate increases. The increase in the stirring rate and the decrease in the D_{32} of the dispersed phase enhanced the mass transfer effect, contributing to the increase in the hydrolysis reaction rate, which agrees with the previous simulation results of the dispersion characteristics of the dispersed phase droplets in the reactor. However, when the stirring rate exceeded 450 r/min, the conversion rate of 2-chlorobenzal chloride per unit of time changed slowly. Considering the hydrolysis reaction efficiency, energy consumption, and other factors, a stirring rate of 450 r/min was more suitable.

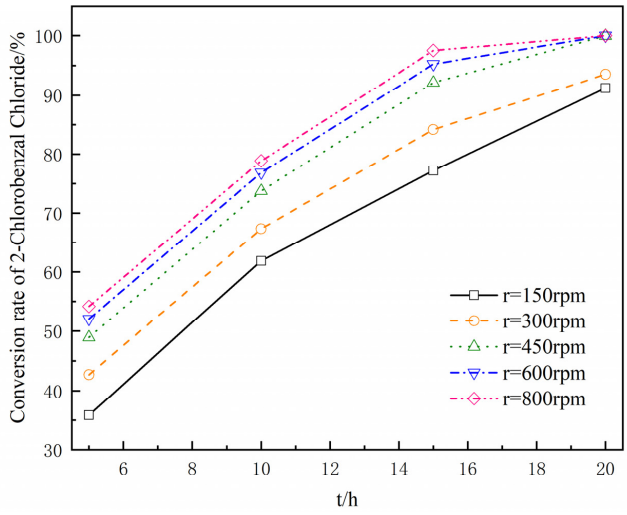

Figure 12. Effect of different stirring speeds on the conversion rate of 2-chlorobenzal chloride.

3.3.3. Effect of Hydrolysis Reaction Time on the Selectivity of 2-Chlorobenzaldehyde

The effect of reaction time on the selectivity of 2-chlorobenzaldehyde at a reaction temperature of 105 °C, a stirring rate of 450 r/min, and a stirring paddle of B_1 was evaluated, and the effect of reaction time on the selectivity of 2-chlorobenzaldehyde is shown in Figure 13. As seen in Figure 13, when the stirring time reached 20 h, the raw material 2-chlorobenzal chloride had been fully converted. The selectivity of 2-chlorobenzaldehyde decreased by continuing to increase the mixing time. The analysis concluded that the hydrolysis reaction time of 20 h is ideal because the product 2-chlorobenzaldehyde was partially oxidized, and 2-chlorobenzoic acid was generated beyond 20 h.

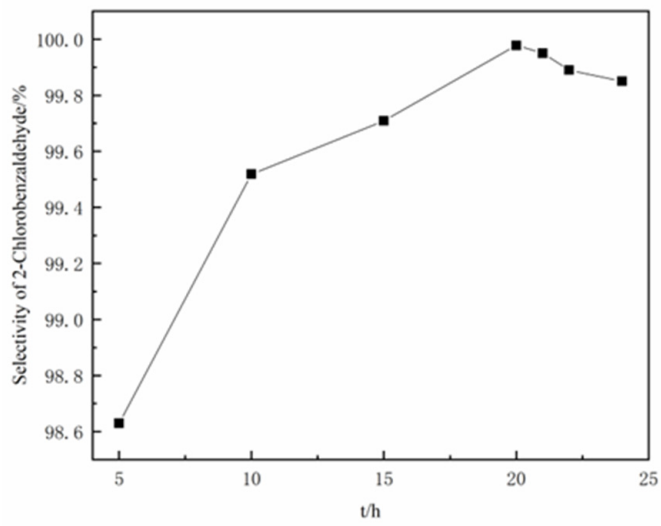

Figure 13. Effect of stirring duration on the selectivity of 2-chlorobenzaldehyde.

3.4. Lab-Scale Validation and Optimization of Intensification Conditions of the Hydrolysis Reaction

Design-Expert 10.0.3 software regression was applied to fit the test data of B_0, B_1, B_2, B_3, and B_4, and the regression equations obtained were as follows.

$$Y_{B_0} = 87.48 + 8.74A + 5.01B - 3.04AB - 1.27A^2 + 0.85B^2 \quad (9)$$

$$Y_{B_1} = 94.99 + 7.46A + 4.17B - 3.4AB - 3.24A^2 + 0.34B^2 \quad (10)$$

Similarly, the regression equations for B_2, B_3, and B_4 are obtained.

$$Y_{B_2} = 93.44 + 8.16A + 5.15B - 2.9AB - 2.92A^2 - 0.37B^2 \quad (11)$$

$$Y_{B_3} = 91.75 + 8.01A + 5.49B - 3.11AB - 2.66A^2 + 0.45B^2 \quad (12)$$

$$Y_{B_4} = 89.41 + 7.79A + 5.59B - 2.84AB - 1.37A^2 + 1.34B^2 \quad (13)$$

Substituting $A = 0$ and $B = 1$ into the regression Equations (9)–(13) and ignoring the errors, we obtain : Y_{B_1} : 100% > Y_{B_2} : 98.22% > Y_{B_3} : 97.69% > Y_{B_4} : 96.34% > Y_{B_0} : 93.34%. From the results of the equation, it can be seen that the highest conversion rate of 2-chlorobenzal chloride was achieved at the reaction time of 20 h, with stirring paddle B_1, and a stirring rate of 450 r/min. Thus, only the experimental results for the three-bladed back-curved impeller B_1 are specifically analyzed here. The design scheme and the results of the test of the hydrolysis of 2-chlorobenzal chloride using the B_1 stirring paddle are shown in Table 5. The test results of stirring paddle B_1 were analyzed by variance using Design-Expert 10.0.3 software, and the analysis results are shown in Table 6.

Table 5. Experimental condition design and results.

Test Number	A Reaction Time	B Stirring Rate	Conversion Rate/%
1	−1	−1	77.21
2	−1	0	84.21
3	−1	1	92.14
4	0	−1	91.21
5	0	0	93.54
6	0	1	99.97
7	1	−1	98.60
8	1	0	99.82
9	1	1	99.92
10	0	0	94.25
11	0	0	95.24
12	0	0	95.09
13	0	0	96.34

Table 6. Variance analysis of reaction conditions.

Variance Source	Degree of Freedom	Sum of Squares	Mean Square	*F*-Value	*p*-Value	Salience
model	5	516.29	103.26	134.73	<0.0001	**
A Reaction time	1	334.21	334.21	436.06	<0.0001	**
B Stirring rate	1	104.25	104.25	136.02	<0.0001	**
AB	1	46.31	46.31	60.42	0.0001	**
A^2	1	28.94	28.94	37.76	0.0005	**
B^2	1	0.32	0.32	0.41	0.5414	
Residuals	7	5.36	0.77			
Misfit	3	0.87	0.29	0.26	0.8531	ns
Pure terror	4	4.5	1.12			
sum	12	521.66				

Note: $p < 0.01$, the difference is very significant, indicated by **; $p > 0.05$, the difference is not significant, expressed by n.

As seen in Table 6, the regression of the model is significant ($p < 0.0001$), the misfit is not obvious ($p > 0.05$), and the model $R^2 = 98.97\%$, $R_{Adj}{}^2 = 98.24\%$. This indicates that the regression results are more satisfactory and reliable. The first-order partial derivatives were solved for the regression equation, in which the maximum value of the conversion rate of 2-chlorobenzal chloride was obtained. The optimal conditions for the two factors were obtained with a reaction time of 21.2 h and a stirring rate of 445.61 r/min, corresponding to a 100% conversion rate of 2-chlorobenzal chloride. The two-factor values were rounded to obtain the corresponding collation values, with a reaction time of 21 h and a stirring rate of 446 r/min. In this case, three replicate experiments were performed to verify that the conversion rate of 2-chlorobenzal chloride was obtained as 100%. Under the stirring action of the B_1 mixing paddle, 2-chlorobenzal chloride was evenly distributed in the reaction kettle and fully contacted with water. The reaction time was reduced, the conversion rate was improved, and the simulation results were reliable, showing that the hydrolysis reactor designed by the main parameters obtained through the simulation is suitable for the hydrolysis of 2-chlorobenzal chloride.

3.5. Industrial-Scale Application of the Optimization Results of Hydrolysis Reaction Conditions in Lab-Scale Tests

Through the verification and optimization of enhanced conditions of the hydrolysis reaction in a lab-scale stirred reactor with a volume of 250 mL, the optimal reaction conditions were screened: a three-bladed back-curved paddle was chosen, the stirring rate was 446 r/min, the mol ratio of oil and water was 1:2.4, the mol ratio of 2-chlorobenzal chloride and phase transfer catalyst of alkyl alcohol amine was 25:1, and the temperature

of the reaction was 105 °C. This condition was applied to an industrial-scale reactor with a volume of 10,000 L, and the results of the industrial-scale experiments are shown in Table 7.

Table 7. Results of the industrial-scale tests.

NO.	Reaction Time/h	Conversion Rate/%	Selectivity/%
1	23	99.986	99.901
2	23	99.975	99.945
3	23	99.972	99.932

Under the optimized reaction conditions, the hydrolysis reaction time was reduced from 36 h to 21 h, which was reduced by 58.33% compared to ordinary conditions using a dichotomous leaf hydrolysis agitator. In addition, the reaction time can be reduced to 63.89% of the pre-intensification level by applying the optimized lab-scale technique to industrial-scale production.

4. Conclusions

1. The dispersion characteristics of droplets in the reactor are simulated and analyzed by using Fluent software, and the dichotomous leaf hydrolysis agitator commonly used in hydrolysis kettles in industrial production is strengthened. The simulation results are also verified by the Sauter mean diameter (D_{32}) measurement experiment of dispersed phase droplets and hydrolysis experiments. The results show that the simulated and experimental results are in good agreement. A log-linear relationship exists between the Sauter mean diameter (D_{32}) of the dispersed phase in different stirred systems and the rotational speed. The three-blade back-curved stirring system possesses a more significant number of tiny droplets and a more uniform particle size, which can enhance the stirrer and mass transfer in the hydrolysis reaction system.
2. A lab-scale hydrolysis reactor is designed and produced based on the scheme of the industrial hydrolysis kettle equipped with a three-bladed back-curved stirring paddle. Under the same conditions, the effect of the hydrolysis reaction is verified, and the process conditions are strengthened. The results show that, compared with the case in the reactor using a dichotomous leaf hydrolysis agitator at the same reaction temperature and catalyst conditions, the reaction time of hydrolysis completion reduced to 58.33% at the lab-scale at the stirring rate of 446 r/min using a three-bladed back-curved stirring paddle. In addition, the reaction time can be reduced to 63.89% of the pre-intensification level by applying the optimized lab-scale technique to industrial-scale production.

Author Contributions: Conceptualization, S.Y. and Y.Z.; methodology, S.Y.; software, S.F. and F.L.; validation, L.D., W.T. and L.N.; formal analysis, J.L.; investigation, F.L.; resources, L.D.; writing—original draft preparation, F.L.; writing—review and editing, S.Y. and J.L.; project administration, S.Y., L.D., W.T. and L.N.; funding acquisition, S.Y., L.D., W.T. and L.N. All authors have read and agreed to the published version of the manuscript.

Funding: This work was supported by participant Shenghu Yan of the Critical Process Reengineering Technology and Demonstration of Hazardous Fine Chemicals Safety Production of the National Key R&D Program (funding number 2021YFC3001100).

Data Availability Statement: Not applicable.

Acknowledgments: We are grateful to the China Salt Changzhou Chemical Co., Ltd. for its provision of the raw material.

Conflicts of Interest: The authors declare no conflict of interest.

References

1. Wu, W.; Shi, S.J.; Chen, W.J. Preparation of o-chlorobenzaldehyde by hydrolysis of o-chlorobenzalchloride. *Sci. Technol. Inf.* **2013**, *34*, 4–6.
2. Nikolić, D.D.; Frawley, P.J. Application of the Lagrangian meshfree approach to modelling of batch crystallisation: Part I—Modelling of stirred tank hydrodynamics. *Chem. Eng. Sci.* **2016**, *145*, 317–328. [CrossRef]
3. Ayranci, I.; Kresta, S.M. Design rules for suspending concentrated mixtures of solids in stirred tanks. *Chem. Eng. Res. Des.* **2011**, *89*, 1961–1971. [CrossRef]
4. Sardeshpande, M.V.; Kumar, G.; Aditya, T.; Ranade, V.V. Mixing studies in unbaffled stirred tank reactor using electrical resistance tomography. *Flow Meas. Instrum.* **2016**, *47*, 110–121. [CrossRef]
5. Montante, G.; Paglianti, A. Gas hold-up distribution and mixing time in gas–liquid stirred tanks. *Chem. Eng. J.* **2015**, *279*, 648–658. [CrossRef]
6. Solsvik, J.; Jakobsen, H.A. Single drop breakup experiments in stirred liquid–liquid tank. *Eng. Sci.* **2015**, *131*, 219–234. [CrossRef]
7. Li, W.L. Study on the relationship between the height of liquid level drop and the shape of the structure of reactor's bottom in multiphase stirred reactor by using CFD. *Fine Spec. Chem.* **2022**, *30*, 53–58.
8. Su, Y.; Yu, P.Q.; Huang, Z.J. Applications of mixing technique in polymerization reaction kettle. *Chem. Propellants Polym. Mater.* **2003**, *1*, 19–23.
9. Svensson, F.J.; Rasmuson, A. PIV measurements in a liquid–liquid system at volume percentages up to 10% dispersed phase. *Exp. Fluids* **2006**, *41*, 917–931. [CrossRef]
10. Drumm, C.; Tiwari, S.; Kuhnert, J.; Bart, H.J. Finite pointset method for simulation of the liquid–liquid flow field in an extractor. *Comput. Chem. Eng.* **2008**, *32*, 2946–2957. [CrossRef]
11. Lamberto, D.J.; Muzzio, F.J.; Swanson, P.D.; Tonkovich, A.L. Using time-dependent RPM to enhance mixing in stirred vessels. *Chem. Eng. Sci.* **1996**, *51*, 733–741. [CrossRef]
12. Lamberto, D.J.; Alvarez, M.M.; Muzzio, F.J. Computational analysis of regular and chaotic mixing in a stirred tank reactor. *Chem. Eng. Sci.* **2001**, *56*, 4887–4899. [CrossRef]
13. Eastwood, C.D.; Armi, L.; Lasheras, J.C. The breakup of immiscible fluids in turbulent flows. *J. Fluid Mech.* **2004**, *502*, 309–333. [CrossRef]
14. Li, X. Design and fatigue study of jacketed reactor. *J. Chifeng Univ. Nat. Sci. Ed.* **2015**, *22*, 198–200.
15. Lu, P.; Li, W.; Zhen, X.W. Numerical simulation on the characteristics of the flow field in glass-lined agitating reactor. *Chem. React. Eng. Technol.* **2016**, *32*, 97–105.
16. Songc, G.; Liy, X.; Wang, W.; Zheng, S. Numerical simulation of hydrate particle size distribution characteristics in pipeline flowing systems. *Chem. Ind. Eng. Prog.* **2018**, *37*, 2912–2918.
17. Lew, A.J.; Buscaglia, G.C.; Carrica, P.M. A note on the numerical treatment of the k-epsilon turbulence model. *Int. J. Comput. Fluid D* **2001**, *14*, 201–209. [CrossRef]
18. Yan, Y.F.; Wang, R.J.; Yang, X.X. CFD simulation of immiscible liquid-liquid dispersion in a stirred tank. *Chem. Ind. Eng.* **2018**, *35*, 70–79.
19. Zhang, H.H.; Wang, T.F. Generality of CFD-PBM coupled model for simulations of gas-liquid bubble column. *CIESC J.* **2019**, *70*, 487–495.
20. Harvey, P.S.; Greaves, M. Turbulent flow in an agitated vessel. Part I: A predictive model. *Trans. Inst. Chem. Eng.* **1982**, *60*, 195–200.
21. Harvey, P.S.; Greaves, M. Turbulent flow in an agitated vessel. Part II: Numerical solution and model predictions. *Trans. Inst. Chem. Eng.* **1982**, *60*, 201–210.
22. Mattei, G.; Vozzi, G. CFD modelling of a mixing chamber for the realization of functionally graded scaffolds. *Comput. Chem. Eng.* **2016**, *84*, 43–48. [CrossRef]
23. Daglas, D.; Stamatoudis, M. Effect of impeller vertical position on drop sizes in agitated dispersions. *Chem. Eng. Technol.* **2000**, *23*, 437–440. [CrossRef]
24. Sechremeli, D.; Stampouli, A.; Stamatoudis, M. Comparison of mean drop size and drop size distributions in agitated liquid-liquid dispersions produced by disk and open type impellers. *Chem. Eng. J.* **2006**, *117*, 11. [CrossRef]